Ising models of undercooled binary system crystallization: Comparison with experimental and pegmatite textures

DON R. BAKER[1],* AND CARMELA FREDA[2],†

[1]Earth and Planetary Sciences, McGill University, 3450 rue University, Montréal, Quebec H3A 2A7, Canada
[2]CNR-Centro di Studio per gli Equilibri Sperimentali in Minerali e Rocce, c/o Dipartimento di Scienze della Terra, Università degli Studi "La Sapienza", P. le Aldo Moro, 5 I-00185 Rome, Italy

ABSTRACT

Simulations of crystal growth in hydrous albite-quartz and albite-orthoclase systems were performed with the Jackson, Gilmer, and Temkin formulation of the Ising model. These simulations demonstrate that at 873 K (approximately 100 K undercooling), comb textures are produced when growth and diffusion probabilities are equivalent. If the growth probability is decreased to 0.1 times that of diffusion, discrete alternating zones of albite and quartz are produced; however, increasing the growth probability to 10 times that of diffusion results in an intergrowth of small domains of albite set in a quartz matrix. At near-liquidus temperatures (973 K), textures similar to those at 100 K undercooling are produced although the crystal-melt interfaces of the comb texture are smoother and the absolute value of the diffusion probability exerts a strong control on the texture, unlike results at 873 K. The textures produced in the simulations with a scale of 10^{-7} m are similar to experimentally produced textures with scales of 10^{-6} to 10^{-4}. The fractal dimension of a comb-textured simulation has been measured and shown to be similar to the fractal dimension of a natural pegmatite with a meter-scale texture. This scaling similarity suggests that these simulations may provide insight into the formation of natural pegmatites despite the 5–7 orders of magnitude difference in scale.

INTRODUCTION

The petrogenesis of granitic pegmatites may be one of the greatest enigmas of igneous petrology at the present time. Pegmatites are typically defined by the presence of large (centimeter scale) to extraordinarily large (several meters across) crystals. The presence of such large crystals suggests that pegmatites cooled slowly and that crystals grew from melts in which diffusion was rapid. However, pegmatites are small bodies, rarely more than 50 m long (Cameron et al. 1949), and commonly intrude cool upper crustal rocks at low temperatures. Consequently, cooling is rapid, requiring only hundreds to thousands of years, at most, to reach solidus temperatures (Chakoumakos and Lumpkin 1990; London 1992; Webber et al. 1997). Additionally, diffusion of silicate components in pegmatite melts is expected to be slow based upon their similarity to granitic compositions (Baker 1991, 1992) and their low liquidus temperatures, near 923 K (Chakoumakos and Lumpkin 1990). If one were to choose a melt composition and conditions of emplacement best suited to the production of small crystals in an intrusive rock, one would choose a pegmatite. Instead, we find that conditions thought to produce small crystals result in exactly the opposite.

Most granitic pegmatite bodies are internally zoned, either symmetrically or asymmetrically, in mineral texture and element distribution. A general zoning pattern has been recognized in many pegmatites. This pattern consists of a lower zone (footwall) composed of a fine grained, albite-rich aplite (in some cases banded or layered); a middle zone that is quartz-rich, in a few cases with open pockets that may contain tourmaline and beryl, quartz, alkali feldspar, and various accessory minerals, and an upper zone (hanging wall) above the quartz core rich in potassium feldspar, commonly graphically intergrown with quartz and typically containing extraordinarily large crystals (Cameron et al. 1949; Jahns 1982). Although this zoning is common it is not ubiquitous and many pegmatites do not display, or only display part of, the zoning pattern (Cameron et al. 1949; Jahns 1982; London 1996).

According to the Jahns and Burnham model (1969) pegmatites are distinguished from typical granites by the presence of a vapor phase (dominated by water) in the former, in addition to melt and crystals; the transition from granitic to pegmatitic texture represents attainment of aqueous vapor saturation of the melt. Jahns and Burnham (1969) argued that pegmatites did not undergo sequential crystallization, but instead experienced eutectic crystallization with near-equilibrium, simultaneous crystallization of quartz, plagioclase, and alkali feldspar in eutectic proportions (Jahns 1982). Jahns and Burnham (1969) attributed the formation of both aplitic albitic rocks in the footwall and giant microcline crystals in the hanging wall to differential solubility of K and Na in an aqueous vapor coexisting with the growing crystals. However they did not provide any explanation of why this vapor did not interact with quartz crystals growing in the center of the pegmatite.

On the basis of experimental studies an alternative explanation for pegmatite formation was proposed by London (London et al. 1989; London 1992, 1996). According to this model the pegmatitic mineral zoning pattern is due to the slow crystallization response of volatile-bearing, but not necessarily

*E-mail: donb@geosci.eps.mcgill.ca
†E-mail: freda@axrma.uniroma1.it

water-saturated, granitic melts to cooling. London determined that experimentally produced textures were affected by the bulk composition of the melt and by the degree of undercooling. Experiments performed at greater undercooling resulted in the formation of coarse-grained, pegmatitic textures whereas those performed at small degrees of undercooling produced fine-grained, granitic textures.

This study presents the results of a theoretical investigation of the creation of crystal textures using Ising models for the crystallization of the binary systems albite-quartz and albite-orthoclase. Although Ising models cannot provide exact simulations of crystal-growth phenomena, they allow investigation of the effects of composition, diffusion coefficients, crystal growth rate, and supercooling on the textural development of binary systems. Results of simulations are extrapolated upward in scale and shown to be similar to previous experimental studies of crystal growth and natural pegmatite textures. Following London's proposal that pegmatite crystallization occurs at significantly undercooled conditions, most simulations were performed at 873 K, approximately 100 K below the eutectic temperature. However, a few simulations were performed at 973 K to compare with textures produced at 873 K.

ISING MODEL OF CRYSTALLIZATION

The Ising model was created in the 1920s to explain the effects of temperature on ferromagnetic behavior (Stanley 1971). The fundamental basis of the model is the concept of a lattice (one dimensional or greater) containing at each point a spin that can be oriented either positively or negatively. Any individual spin only interacts with its nearest neighbors on a lattice; the energy of the system is determined by interactions between each spin and its neighbors and is described by the Hamiltonian, H:

$$H = -J \sum_{ij} \sigma_i \sigma_j \qquad (1)$$

where J is the interaction energy between spins, and σ_i and σ_j are spins with the values of $+1$ or -1 corresponding to positive and negative spin orientations (Stanley 1971; Ross 1991). The transition frequency (or transition probability) of a spin from one orientation to another is determined by the exponential of the opposite of the Hamiltonian divided by Boltzmann's constant multiplied by the temperature (Stanley 1971; Ross 1991). At low temperatures virtually all spins are aligned in either the positive or negative orientation and the object is magnetic; at high temperatures the spin orientations are random and no magnetic behavior is observed. Although a gross simplification of natural systems, the Ising model has been applied successfully to modeling gas-liquid phase transitions and the crystallization of binary alloys, in addition to magnetic phase transitions (Stanley 1971; Ross 1991).

The version of the Ising model used in this study to investigate the crystallization of the albite-quartz and albite-orthoclase binaries is the spin-1 Ising model of Jackson et al. (1995), hereafter referred to as the JGT model. The JGT model has been demonstrated to reproduce experimental results in the silicon-bismuth binary system (Jackson et al. 1996; Beatty and Jackson 1997). This model contains four "spins," one each for the components i and j in either melt or crystal. A negatively

oriented "spin" is considered to be in the liquid phase and a positively oriented one is in the crystalline phase. The model calculates the crystallization of a supercooled melt in a binary system on a square lattice (i.e., four nearest neighbors in both crystal and melt) at constant temperature. Three transition frequency expressions are used for the calculations: one for addition of adatoms (which in this work are either quartz, albite, or orthoclase molecules) to the growing crystal; one for removal of adatoms from the crystal; and one for diffusion of adatoms in the melt. The frequency of conversion of adatoms from melt to crystal, ν_i^{LS}, is given by (Jackson et al. 1995; Beatty and Jackson 1997):

$$\nu_i^{LS} = \nu \exp\left(-\frac{\Delta S}{k}\right) \exp\left(-\sum_j \frac{\varepsilon_{ij}}{kT}\right) \qquad (2)$$

where ν is a normalizing frequency based upon diffusion in the melt, ΔS is the normalized entropy of melting, k is the Boltzmann constant, ε_{ij} is the bond energy between a chosen adatom and its neighbor atom of either type i or j, and T is the temperature in kelvins. The frequency at which adatoms detach from the crystal and enter the melt, ν_i^{SL}, is given by:

$$\nu_i^{SL} = \nu \exp\left(-\sum_j \frac{\varepsilon_{ij}}{kT}\right). \qquad (3)$$

Following Beatty and Jackson (1997) diffusion of adatoms in the melt toward the growing crystal was modeled as a simple exchange of two components on different lattice sites in the melt with a frequency, ν, determined by:

$$\nu = \frac{2Dd}{a^2} \qquad (4)$$

where D is the diffusion coefficient, d is the dimensionality (2 in the present study), and a is the "jump distance," which is estimated to be 1 nm (Baker 1992). This frequency provides the normalizing value, n, in the equations for the attachment and detachment of an adatom to the growing crystal in JGT model (Beatty and Jackson 1997).

Crystallization is modeled using the Monte Carlo technique (Heermann 1986) on a lattice with periodic boundary conditions such that when an adatom diffuses to the right of the column at the right-hand boundary, it diffuses into the first column at the left-hand boundary. At each point on the lattice the computer determines which composition, i or j, is present and whether the adatom is in the liquid or crystalline state. If the adatom is liquid, the diffusion frequency is calculated and compared to a random number; diffusion occurs when the frequency is greater than the random number. If the liquid adatom is in contact with one or more crystalline adatoms, the attachment frequency is calculated and compared to a random number; the adatom is converted from liquid to solid if the frequency is greater than the random number. If the adatom at the lattice site is solid and totally surrounded by solid adatoms nothing occurs. If, instead, one of the four nearest-neighbor adatoms is liquid, the detachment frequency of the adatom under consideration is calculated and compared to a random number; if the detachment frequency is greater than the random number, the adatom is converted from a solid to a liquid. Note that no diffusion is allowed in the crystalline phases. A single sweep is composed of performing these calculations at each lattice point in the model. A typical model in this study is composed of 5×10^4

to 3×10^6 sweeps of a 300×150 lattice of which 10 rows were initially crystalline albite and the others were melt. These conditions were chosen as a compromise between the computational time necessary for calculation of substantial amounts of crystallization and the desire to have a model as large as possible. All models were constrained to have one row of crystalline material at the bottom and one row of molten material at the top of the lattice. The simulations do not include any gravitational effects; thus, any simulated growth upward from the seed crystal at the base can also represent growth downward from the top.

Pressure, temperature and water concentration in the models

Modeling the crystallization of albite-quartz and albite-orthoclase binaries was performed at temperatures of 873 K and 973 K. The temperature of 973 K is the eutectic temperature in the albite-orthoclase system at 500 MPa, water-saturated conditions, and is close to the estimated eutectic temperature in the water-saturated, albite-quartz binary at 400 MPa (Ehlers 1972). The choice of the eutectic temperature reflects the observation that pegmatite compositions commonly plot close to the eutectic in the system albite-orthoclase-quartz (London 1996) and should be modeled as eutectics in the binary systems. Eutectic temperatures near 500 MPa were chosen to reflect magmatic conditions at mid-crustal depths. The temperature of 873 K was chosen to represent an undercooling of 100 K experienced by a pegmatite at its contact with surrounding country rocks that are 200 K cooler than the intruding pegmatite (cf., Chakoumakos and Lumpkin 1990).

The models do not explicitly investigate the role of water in the crystallization of feldspars and quartz. However, because water affects the melting temperatures of minerals, and the bond energies used in the models are determined from mineral liquidi (discussed below), water affects the model indirectly. This study only investigated crystallization from water-saturated melts to constrain the effects of undercooling and differing diffusion and growth rate transition probabilities on the textures produced. Importantly, no free fluid is present in these models.

Diffusion in the melt

Chemical diffusion coefficients used for the calculation of the frequency of diffusive exchange, , were chosen to span the possible range of values present in a pegmatitic melt at temperatures between 873 and 973 K. The maximum values for are calculated from the chemical diffusion coefficients of Na and K determined by Freda and Baker (1998) in hydrous alkali feldspar melts extrapolated to the model temperatures. The minimum values for were calculated from viscosities of granitic melts with the Eyring equation and correspond to Si-Al interdiffusion (Baker 1992).

Attachment and detachment frequencies

The normalizing frequency, , in the expressions for both attachment and detachment is related to the diffusion probability, , and both are in s^{-1}. Although the relationship between diffusion in the melts and the crystallization kinetics of plagioclase from hydrous melts has been demonstrated (Muncill and Lasaga 1988), the exact relationship between the diffusion frequency and the attachment and detachment frequencies remains experimentally unconstrained. Therefore, modeling was performed with equal to three values: the diffusion probability, 10 times the diffusion probability and 0.1 times the diffusion probability. The use of three different values allows investigation of how the relationship between diffusion and crystal growth affects the crystallization behavior of the system even though the exact relationship remains unknown.

The correspondence between sweeps and elapsed time in a simulation is complicated when is not equal to 1 because the time of a diffusive event and of a growth or dissolution event are not the same. In this case an average time can be computed by storing the number and type of events that occur during each simulation. Currently we are not interested in the exact duration of the simulations. However, the durations can be roughly estimated by multiplying the time step used for the diffusion probability by the number of sweeps. These approximate times are on the order of milliseconds to hundreds of seconds.

Bond and interaction energies for crystallization model

To create a microscopic model for the crystallization of two minerals (i and j) from a melt in a binary system it is necessary to specify the interaction (bond) energy, $_{ij}$, between two i molecules, between two j molecules, and between i and j molecules in both molten and crystalline phases. For simplicity, the interaction energies between all components in the melt have been taken to be 0 (Beatty and Jackson 1997). The interaction energy of each end-member bond energy (i-i or j-j) can be established through knowledge of the melting temperatures of crystals of pure i and pure j at the conditions of interest (pressure, water concentration in the melt, etc.). This initial value for the determination of the bond energy is the enthalpy of crystallization of the crystal divided by Avogadro's number. This value is modified until the model melting temperature of the pure end-member crystal is within ±10 K of the real melting temperature. In this study three end-members were considered, albite, orthoclase, and quartz, and their bond energies determined for water-saturated melting at 500 MPa. These values in terms of J/k for albite, orthoclase, and quartz are 1300, 1430, and 1800, respectively.

Interaction energies between i and j end-members in the crystals are based upon a regular solution model for the solid. Although such a model is a simplification of the real interactions between the end-members (Navrotsky 1994), it is sufficient for the present purposes. The symmetric Margules parameter, W_G, is calculated from the estimated consolute temperature of the solvus between i and j (Navrotsky 1994). This value is then scaled using the enthalpies of melting of i and j and the bond energies necessary to reproduce the melting temperatures of the pure end-members. The estimated consolute temperature of the solvus between albite and orthoclase at 500 MPa is 1048 K which yields a W_G of 16.6 kJ/mol. This value was divided by the average of the enthalpies of melting for albite and orthoclase, and then multiplied by the average of $_{ij}$ for albite and orthoclase to calculate the normalized i-j interaction energy, 369 J/k. There is no measured solvus between either orthoclase or albite and quartz at 500 MPa. However, Navrotsky et al. (1982) summarize earlier studies of the amounts of excess silica in albite and orthoclase. These data indicate that the solid solution of quartz in

feldspars (and vice versa) may be approximated with a solvus exhibiting a consolute temperature far in excess of 2400 K that, when normalized, produces an *i*-Quartz (where *i* is either albite or orthoclase) interaction energy that is at least 1000 J/k; this value was used in the simulations presented herein.

Entropy of crystallization

The value of S/k used in all calculations was 5. This estimate is similar to that of Beatty and Jackson (1997) and is based upon the bond-bond energy divided by the temperature of melting of the pure end-member phase. Although the estimate is not exact, small deviations from this value do not have any significant effect on the simulations of this study.

MODELING RESULTS

Crystallization far below the liquidus

Simulations at 873 K represent conditions approximately 100 K below the water-saturated albite-quartz eutectic at 400 MPa. Simulations at the eutectic composition, $X_{Albite} = 0.3$ on an anhydrous basis, were performed on a 300 × 150 lattice with the first 10 rows composed of a pure albite seed crystal. A time step of 10 ns was used in simulations with a rapid alkali interdiffusion coefficient, 5.9 ×10⁻¹³ m²/s, and a step of 0.01 s was used in simulations with a slow Si-Al interdiffusion coefficient, 1.7 × 10⁻¹⁷ m²/s, for the calculation of diffusion and growth probabilities per time step. The simulations presented below are either in the albite-quartz or albite-orthoclase binary systems. Simulations of the quartz-orthoclase binary system produced results indistinguishable from those of the albite-quartz binary and are not shown.

Figure 1 presents a time series during crystallization when the growth probability equals the diffusion probability, and diffusion is rapid. Although the simulation begins with a smooth crystal-melt interface, the growing quartz dominates the simulation and rapidly develops a comb structure with the long dimension perpendicular to the horizontal seed crystal. The growing quartz traps melt inclusions of albite composition that crystallize during later steps in the simulation. The individual domains of quartz and albite are almost pure end-member phases with little solid solution, as demanded by the high albite-quartz interaction energy in the model.

Increasing the probability of growth relative to diffusion by 10 times results in a change from a comb texture to a much finer-grained one with smaller domains of quartz and albite that are densely intergrown one with another (Fig. 2b). If the probability of growth is 0.1 times that of diffusion, the texture changes into one of discrete zones with nearly pure quartz followed by albite (Fig. 2c). As discussed above, the exact durations of the simulations were not determined, but estimates of the duration based upon the number of sweeps multiplied by the time step demonstrates that reducing the growth probability by a factor of ten decreases growth rates by a factor of ten as expected.

Simulations using the slow diffusion values produced textures virtually identical to those discussed above (Fig. 3). Note that crystallization was complete before the simulation with equal growth and diffusion probabilities reached 100,000 sweeps, which prevents any estimation of crystal growth rates
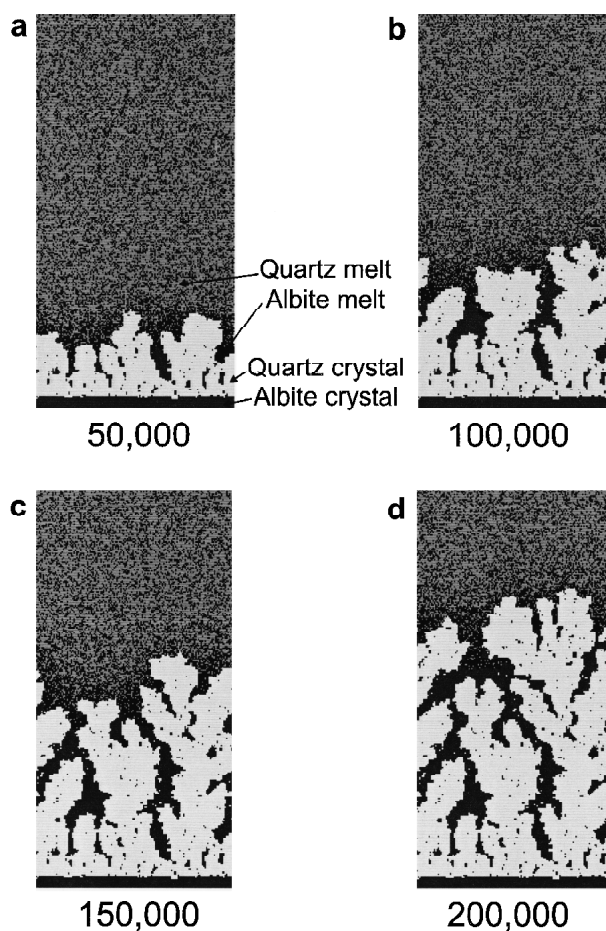

FIGURE 1. Ising model simulation of albite and quartz crystal growth for a eutectic composition, $X_{Albite} = 0.3$, anhydrous basis, at 873 K (approximately 100 K below the equilibrium crystallization temperature when water-saturated at 400 MPa). Diffusion in this simulation is based upon Na-K interdiffusion coefficients in feldspar melts (5.9 × 10⁻¹³ m²/s). In this and all other simulations, dark gray and black represents crystalline and molten albite, respectively; white and light gray represents crystalline and molten quartz, respectively; the number of Monte Carlo sweeps, which is proportional to the elapsed time in the simulations, is given under each panel in the diagram. See text for further discussion.

for these conditions. When growth and diffusion probabilities are equal, a comb structure is observed (Fig. 3a). When the growth probability is only 0.1 times that of diffusion (Fig. 3b) large discrete zones of quartz and albite grow, as seen in Figure 2c at higher diffusivities. A simulation involving a higher growth probability was not performed on a 300 × 150 lattice, but smaller simulations on 150 ×150 lattices (not shown) demonstrate the same results as seen for the slow diffusion values.

The effect of composition when growth and diffusion probabilities are equal is striking. If the composition is changed from $X_{Albite} = 0.3$ to $X_{Albite} = 0.7$ (anhydrous basis), the texture changes from the comb structure shown in Figure 1 to a structure similar to that observed in the eutectic composition when the growth probability is 10 times that of diffusion (Fig. 2b), but with larger domains of albite and quartz (Fig. 4a). The crys-
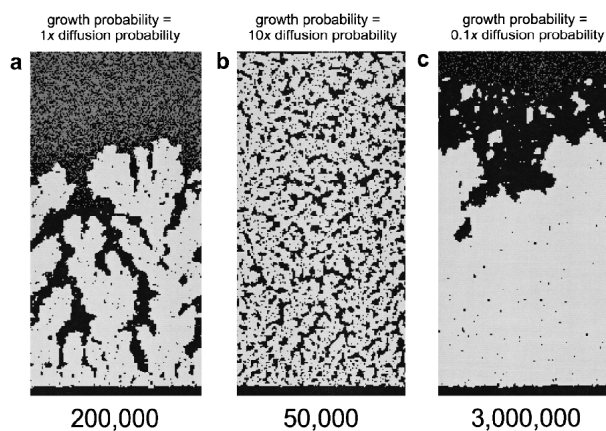
growth probability = 1x diffusion probability

growth probability = 10x diffusion probability

growth probability = 0.1x diffusion probability

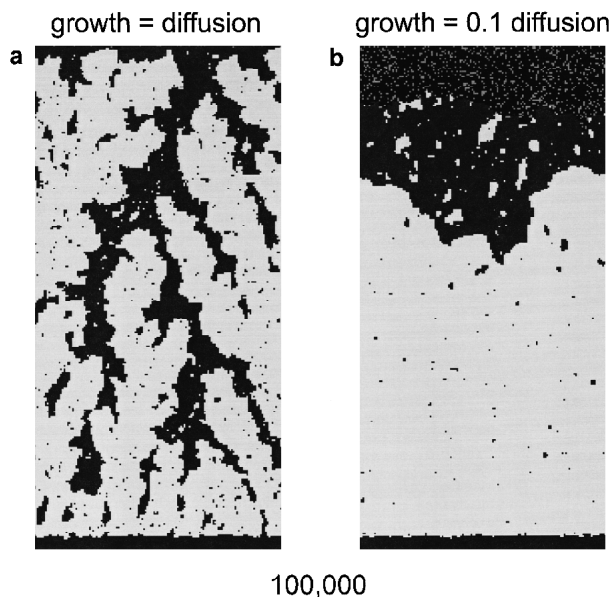a   b   c

200,000   50,000   3,000,000

FIGURE 2. The effect of relative probabilities (frequencies) of growth and diffusion on the structures produced from an albite-quartz eutectic composition crystallized at 873 K, when the absolute value of diffusion is that of Na-K in feldspar melts (5.9×10^{-13} m^2/s).

growth = diffusion   growth = 0.1 diffusion

a   b

100,000

FIGURE 3. The effect of relative probabilities (frequencies) of growth and diffusion on the structures produced from an albite-quartz eutectic composition crystallized at 873 K, when the absolute value of diffusion is that of Si-Al interdiffusion in a granitic melt (1.7×10^{-17} m^2/s). Note the similarity between Figures 2a and 3a and 2c and 3b, respectively.

tallization of the albite-orthoclase eutectic composition, X_{Albite} = 0.66 (anhydrous basis) was modeled at 873 K using alkali interdiffusion coefficients and equal diffusion and growth probabilities. The resulting structure is composed of an intimate mixture of albite and orthoclase with a smooth melt-crystal interface (Fig. 4b). The great difference between the structures produced in the albite-quartz and albite-orthoclase simulations is due to the high interaction energy between albite and quartz, which results in domains of nearly pure end-member phases rather than an intimate mixture.
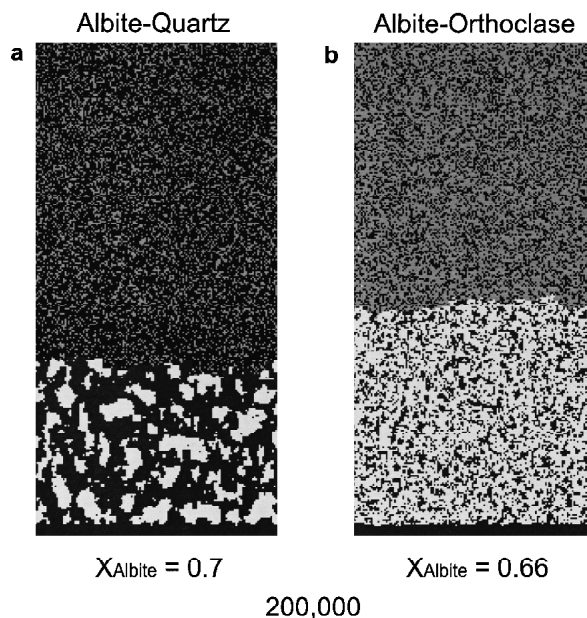

Albite-Quartz   Albite-Orthoclase

a   b

X_{Albite} = 0.7 X_{Albite} = 0.66

200,000

FIGURE 4. The effect of composition on the structures produced by crystallization at 873 K when growth probability equals diffusion probability and the diffusion coefficient is that of Na-K in feldspar melts (5.9×10^{-13} m^2/s). In the albite-orthoclase simulation, dark gray and black represent crystalline and molten orthoclase, respectively; white and light gray represent crystalline and molten albite, respectively.

These simulations demonstrate that the important controls on the textures produced at 873 K are the composition and the relative probabilities of diffusion and growth, not the absolute values. Changing the relative probabilities of diffusion and growth result in drastically different textures of quartz and albite at approximately 100 K below the equilibrium crystallization temperature.

Crystallization near the liquidus

A small number of simulations were performed at 973 K for comparison with those at 873 K. These simulations were performed on a 300 × 150 lattice with the first 10 rows composed of a pure albite seed crystal and the eutectic composition in the albite-quartz system. A time step of 10 ns was used in simulations with a rapid alkali interdiffusion coefficient, 3×10^{-12} m^2/s, and a time step of 0.01 s was used with a slow Si-Al interdiffusion coefficient, 1.5×10^{-16} m^2/s.

The overall texture is similar at both temperatures when the diffusion probability equals the growth probability and the alkali interdiffusion coefficient is used to calculate (Fig. 5a). The comb structure seen at 873 K is present, but crystals grown at 973 K have smoother interfaces with the melt compared to those at 873 K (Fig. 2a). Reducing the growth probability to 0.1 times that of diffusion results in the formation of large masses of quartz crystals, but no significant crystallization of albite (Fig. 5b) as observed in the 873 K simulation (Fig. 2c). However, albite-enriched regions of melt exist at the edges of the growing quartz crystals and, if the simulation had been performed for a longer time, a domain of crystalline albite would probably have been produced as seen at 873 K.
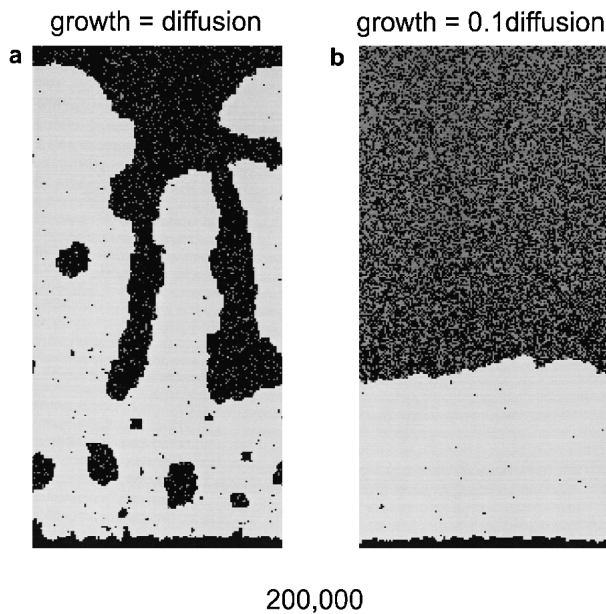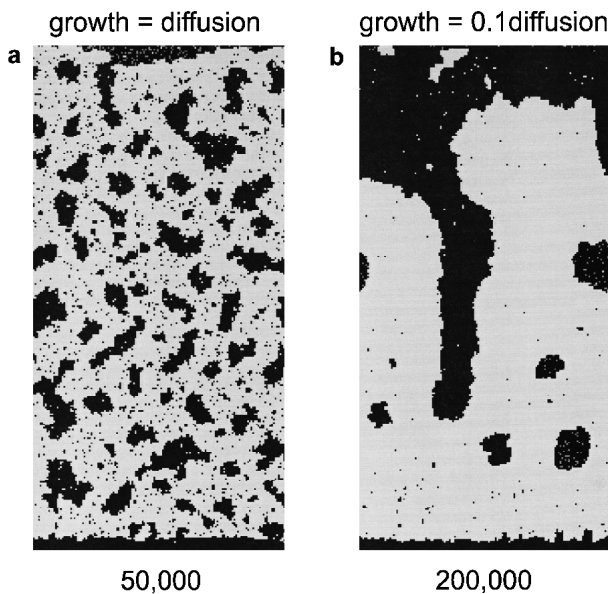
FIGURE 5. The effect of relative probabilities (frequencies) of growth and diffusion on the structures produced from an albite-quartz eutectic composition crystallized at 973 K, when the absolute value of diffusion is that of Na-K in feldspar melts (3.0×10^{-12} m^2/s).

FIGURE 6. The effect of relative probabilities (frequencies) of growth and diffusion on the structures produced from an albite-quartz eutectic composition crystallized at 973 K, when the absolute value of diffusion is that of Si-Al interdiffusion in a granitic melt (1.5×10^{-16} m^2/s).

Decreasing diffusion in the melt to the low value at 973 K results in a dramatic change in the crystallized texture when diffusion and growth probabilities are equal (Fig. 6a). No semblance to a comb structure is observed when growth and diffusion probabilities are equal. Instead, the texture is composed of moderate-sized domains of crystalline albite set in a quartz

matrix. This simulation resembles that produced at 873 K when the growth probability was 10 times the diffusion probability (Fig. 2b), except that the domains of crystalline albite are larger. Reducing the growth probability to 0.1 times the diffusion probability results in a comb texture (Fig. 6b) similar to that formed at 873 K (Fig. 2a). The near-total crystallization of both 973 K simulations in Figure 6 is due to the long time step used, 10^{-2} s, which results in estimated simulation durations of hundreds of seconds. In all 973 K simulations the initial albite seed crystal partially dissolved early in the simulation even though albite crystallizes at later times.

The near-liquidus crystallization textures of the simulations at 973 K are affected by the absolute value of diffusion as well as by the relative probabilities of diffusion and growth. However, the general results at 973 and 873 K remain the same, the lower the growth probability relative to diffusion the larger the single crystal domains of quartz and albite.

DISCUSSION
Comparison with experimental microtextures

The control of crystal textures by undercooling, composition, and the relative probabilities (which are equivalent to rates) of crystallization and diffusion in the melt identified by the simulations is consistent with experimental studies, despite the difference in scale between simulations experiments (10^{-7} m vs. typically 10^{-6} to 10^{-4} m). The effects of undercooling and composition have been demonstrated experimentally in studies of crystal growth in geological systems that have produced textures similar to those in the simulations (e.g., Fenn 1977, 1986; Lofgren 1980; London 1992). Good examples of this similarity between modeling results and experiments are in Fenn (1986) and London (1992). Fenn (1986) contains numerous photographs of micrometer-sized quartz-albite intergrowths formed by undercooled crystallization of natural pegmatite compositions. Figures 8b and 8c of London (1992) display feldspar-quartz intergrowths whose texture is mimicked by the simulation in Figure 1d of this contribution despite the 2 orders-of-magnitude difference in scale between experiment and simulation. Although the similarities between experimental and simulated microtextures is great, rigorous quantitative comparison using fractal dimensions (see below) failed because we could not find any published photographs of experimental textures with the necessary resolution.

Although much has been learned from experimental studies on crystal growth, the simulations for the eutectic composition provide additional insight into the experimental observations, despite our current inability to make quantitative scaling comparisons through the use of fractals. The simulations at 100 K undercooling indicate that, although the absolute values of diffusion and growth probabilities affect growth rates, they are unimportant in controlling texture. However, changes in the relative values of growth and diffusion rates exert significant effects on the texture and growth rate. At near-liquidus conditions, the absolute values of growth and diffusion probabilities affect the textures produced as well as the growth rates. These observations of the simulations can be used to investigate some of the experimental observations on crystal growth even though experimental and simulation systems are not compositionally identical.

The experimental observation that crystals grown at near-liquidus conditions are euhedral with no morphological instability (e.g., Lofgren 1980) combined with simulations at 973 K (Figs. 5 and 6) suggest that growth probabilities in experiments are significantly lower than those of diffusion at these conditions. The probability of growth relative to diffusion necessary for morphological stability appears to be either <1, estimated from Figure 5 with rapid diffusion coefficients in the simulations, or <0.1, estimated from Figure 6 when the slower diffusion coefficients are used in the simulations.

The loss of morphological stability when crystallization occurs at significant undercoolings (100 K) might be due to an increase in the probability of growth relative to that of diffusion based upon simulation results presented Figures 1, 2, and 3. This relative increase is due to a combination of higher Gibbs free energies of crystallization with increasing undercooling (e.g., Dowty 1980) and decreasing diffusion coefficients at lower temperatures (e.g., Baker 1991). Simulation results indicate that to prevent morphological instability, the growth probability must be maintained at a value less than approximately 0.5 that of the diffusion probability.

Fenn (1977) demonstrated that feldspar growth rates are strongly affected by H_2O concentrations in the melt. His experiments demonstrated that at an undercooling of 100 K, an increase in H_2O from 5.4 to 9 wt% decreases sodic feldspar growth rates by a factor of 2.5. A similar effect was observed by Muncill and Lasaga (1988) in their experimental study of albite-anorthite growth kinetics from water-saturated melts at 200 and 500 MPa. Because increasing H_2O concentrations always result in higher diffusivities in granitic melts (Baker 1991; Freda and Baker 1998), the simulations suggest that the decrease in observed growth rates is due to the depression of the growth probability relative to that of diffusion by H_2O addition. Such behavior with increasing H_2O concentration may result in a return to morphological stability, but this has not been observed yet. The simulation results combined with the experimental results of Fenn (1977) and Muncill and Lasaga (1988) indicate that significantly undercooled melts with low H_2O contents should produce crystals with morphological instabilities. Thus, higher H_2O concentrations would lead to the decreasing growth rates that are expected to produce morphologically stable crystals, such as those possibly existing in alternating domains as in Figures 2 and 3.

An increase in growth probability to 10 times that of diffusion produces smaller crystals (Fig. 2b). Although crystallographic controls on the orientation of growing quartz and albite are not included in the square lattice simulations, the structure produced is similar to graphic granite, which Fenn (1986) produced experimentally by crystallization of hydrous pegmatitic compositions at undercoolings of 100–165 K below the liquidus. This structure appears in all albite-quartz simulations at 873 K in which the growth probability is 10 times that of diffusion and is not dependent upon composition.

The most exciting result of the simulations is the prediction that relatively small changes in the probability of growth relative to diffusion can have significant effects on the microtextures produced in experiments.

Comparison with pegmatite textures

The Ising model simulations create textures that are remarkably similar to those observed in pegmatites. However, each adatom in the simulation (equivalent to a pixel in the figures) is approximately 1 nm. Therefore the textures produced in the simulations have dimensions on the order of 10^{-7} m whereas the mineralogical zoning seen in pegmatites is 5–7 orders of magnitude larger (centimeters to meters in size). Despite qualitative similarities between simulations and natural textures, and the observation that pegmatitic fabrics exist on scales that vary from centimeters to meters in size, or >2 orders of magnitude (Cameron et al. 1949; Jahns and Burnham 1969; Jahns 1982), application of the modeling results to natural systems requires scaling the simulation textures up these many orders of magnitude. Although we recognize that such scaling is fraught with potential problems, we cannot resist our curiosity and make the comparison between microscopic and macroscopic textures.

Quantitative comparison between simulated and natural textures can be achieved through determination of the fractal dimensions of both types of textures (Fowler 1995). Fowler (1995) summarized his previous research on the fractal nature of quench crystals in basaltic rocks and demonstrated that simple fractal models using adatoms can be scaled from atomic to cm-scale dimensions and accurately reproduce observed textures.

We evaluated the fractal dimension of the texture of quartz crystals developed in Figure 1d and compared this dimension to those of natural pegmatite fabrics with meter-scale textural variations displayed in Figures 3a and 3b of Chakoumakos and Lumpkin (1990). The photographs of Chakoumakos and Lumpkin (1990) were used because they were the only published ones of pegmatite textures with sufficient resolution for fractal analysis. The fractal dimension was determined by converting the image to a black (quartz crystals) and white (all other phases) image then finding the edges of the crystals using Corel Photopaint. This edge was used to find the fractal dimension of the texture through use of the box-counting technique (Schroeder 1991; Fowler 1995) as implemented by the software package Beniot 1.1 (TruSoft International Inc., St. Petersburg, Florida, U.S.A.). In all cases the box edge length varied by approximately two orders of magnitude (cf. Fowler 1995).

The fractal dimensions of the simulations and the natural textures were similar, but not always within error of each other. The simulation (Fig. 1d) had a fractal dimension of 1.900 ± 0.001 (1 standard deviation error) whereas the natural textures of Figure 3a and 3b of Chakoumakos and Lumpkin (1990) had dimensions of 1.899 ± 0.002 and 1.907 ± 0.002, respectively. Importantly, all measured data formed a linear trend when the log of the number of black pixels in the box was plotted against the log of the box edge length and no evidence of "cross-over" from fractal to constant density distribution was observed (cf. Fowler 1995). The similarity in fractal dimension between simulation and nature encourages us to apply our simulations to the investigation of natural pegmatite fabrics. However, these fractal measurements are preliminary and we are currently seeking photographs of pegmatite textures for more detailed fractal comparisons of nature and simulation.

The albite-quartz simulations performed at 873 K, an un-

dercooling of approximately 100 K, with the eutectic composition reproduce many of the textural features seen in pegmatites. When growth and diffusion probabilities are equal, the simulations produce comb structures (Figs. 2a and 3a) that are characteristic of anisotropic fabrics in pegmatites (London 1992). This result is produced in simulations involving either albite-quartz or orthoclase-quartz (not shown) binary systems. This texture can be found in natural pegmatites growing away from contacts with the host rocks (Jahns and Burnham 1969; Jahns 1982; London 1992). In contrast, albite-orthoclase and albite-quartz compositions far from that of the eutectic do not produce such structures (Fig. 4). The absence of the comb structure in the albite-orthoclase binary is due to the low interaction energy between these two crystals, which allows significant solubility of one within the other. The absence of the structure in the albite-quartz simulation when $X_{Albite} = 0.7$ suggests that quartz must be the dominant anhydrous component in the melt. Note that on a weight percent basis, however, albite is the dominant species in both compositions studied in the albite-quartz binary.

The formation of large domains of pure quartz and albite in the simulations occurs when the growth probability is <0.5 times that of diffusion (Figs. 2c and 3b). The texture in these simulations is similar to the alternating layers composed dominantly of feldspar or quartz that are found in the footwall of some pegmatites (Cameron et al. 1949; Jahns and Burnham 1969; Jahns 1982; London 1992, 1996). The formation of these large domains in the simulations is also reminiscent of large masses of nearly pure quartz seen in the cores of pegmatites (Cameron et al. 1949; Jahns and Burnham 1969; Jahns 1982; London 1992, 1996). The change in the relative probabilities of diffusion and growth in the natural case can be explained by increases in melt H_2O concentrations due to crystallization of anhydrous crystals. This increase results in an apparent diminution of the growth probability relative to that of diffusion as discussed above in the comparison between simulations and the experiments of Fenn (1977) and Muncill and Lasaga (1988), and discussed by London (1992, 1996) for natural pegmatites.

These simulations are consistent with the hypothesis of London (1992, 1996) in which the formation of pegmatites may occur at high undercoolings from water-undersaturated magmas. These simulations demonstrate that textures, albeit microtextures, similar to those produced in experiments and in natural pegmatites can be formed in the absence of a hydrous vapor. For eutectic compositions at an undercooling of 100 K, small changes in the relative probabilities (rates) of growth and diffusion produce very different textures in the Ising model simulations investigated.

ACKNOWLEDGMENTS

REFERENCES CITED

Baker, D.R. (1991) Interdiffusion of hydrous dacitic and rhyolitic melts and the efficacy of rhyolite contamination by dacitic enclaves. Contributions to Mineralogy and Petrology, 106, 462–473.
—— (1992) Interdiffusion of geologic melts: calculations using transition state theory. Chemical Geology, 98, 11–21.
Beatty, K.M. and Jackson, K.A. (1997) Orientation dependence of the distribution coefficient obtained from a spin-1 Ising model. Journal of Crystal Growth, 174, 28–34.
Cameron, E.N., Jahns, R.H., McNair, A.H., and Page, L.R. (1949) Internal structure of granitic pegmatites, 115 p. Economic Geology Monograph, 2.
Chakoumakos, B.C. and Lumpkin, G.R. (1990) Pressure-temperature constraints on the crystallization of the Harding pegmatite, Taos County, New Mexico. Canadian Mineralogist, 28, 287–298.
Dowty, E. (1980) Crystal growth and nucleation theory and numerical simulation of igneous crystallization. In R.B. Hargraves, Ed., Physics of Magmatic Processes, 419–485 p. Princeton University Press, Princeton.
Ehlers, E.G. (1972) The Interpretation of Geological Phase Diagrams, 280 p. W.H. Freeman, San Francisco.
Fenn, P.M. (1977) The nucleation and growth of alkali feldspars from hydrous melts. Canadian Mineralogist, 15, 135–161.
—— (1986) On the origin of graphic granite. American Mineralogist, 71, 325–330.
Fowler, A.J. (1995) Mineral crystallinity in igneous rocks: Fractal method. In C.C. Barton and P.R. LaPointe, Eds., Fractals in the Earth Sciences, 237–249 p. Plenum Press, New York.
Freda, C. and Baker, D.R. (1998) Na-K interdiffusion in alkali feldspar melts. Geochimica et Cosmochimica Acta, 62, in press.
Heermann, D.W. (1986) Computer Simulation Methods in Theoretical Physics, 145 p. Springer-Verlag, Berlin.
Jackson, K.A., Gilmer, G.H., and Temkin, D.F. (1995) Monte Carlo simulation of the rapid crystallization of bismuth-doped silicon. Physical Review Letters, 75, 2530–2533.
Jackson, K.A., Gilmer, G.H., Temkin, D.F., and Beatty K.M. (1996) Microsegregation far from equilibrium. Journal of Crystal Growth, 163, 461–469.
Jahns, R.H. (1982) Internal evolution of pegmatite bodies. In P. Cerny, Ed., Granitic Pegmatites in Science and Industry, 293–327 p. Mineralogical Association of Canada Short Course Handbook Volume 8, Mineralogical Association of Canada, Winnipeg.
Jahns, R.H. and Burnham, C.W. (1969) Experimental studies of pegmatite genesis: I. A model for the derivation and crystallization of granitic pegmatites. Economic Geology, 64, 843–864.
Lofgren, G. (1980) Experimental studies on the dynamic crystallization of silicate melts. In R.B. Hargraves, Ed., Physics of Magmatic Processes, 487–551 p. Princeton University Press, Princeton.
London, D. (1992) The application of experimental petrology to the genesis and crystallization of granitic pegmatites. Canadian Mineralogist, 30, 499–540.
—— (1996) Granite pegmatites. Transactions of the Royal Society of Edinburgh Earth Sciences, 87, 305–319.
London, D., Morgan, G.B. VI, and Hervig, R.L. (1989) Vapor-undersaturated experiments in the system macusanite-H_2O at 200 MPa and the internal differentiation of granitic pegmatites. Contributions to Mineralogy and Petrology, 102, 1–17.
Muncill, G.E. and Lasaga, A.C. (1988) Crystal-growth kinetics of plagioclase in igneous systems: Isothermal H_2O-saturated experiments and extension of a growth model to complex silicate melts. American Mineralogist, 73, 982–992.
Navrotsky, A. (1994) Physics and Chemistry of Earth Materials, 417 p. Cambridge.
Navrotsky, A., Capobianco, C., and Stebbins, J. (1982) Some thermodynamic and experimental constraints on the melting of albite at atmospheric and high pressure. Journal of Geology, 90, 679–698.
Ross, C.R. II (1991) Ising models and geological applications. In J. Ganguly, Ed., Diffusion, Atomic Ordering and Mass Transport, 51–90 p. Springer-Verlag, New York.
Schroeder, M. (1991) Fractals, Chaos, Power Laws, Minutes from an Infinite Paradise, 429 p. Freeman, New York.
Stanley, H.E. (1971) Introduction to Phase Transitions and Critical Phenomena, 308 p. Oxford University Press, New York.
Webber, K.L., Falster, A.U., Simmons, W.B., and Foord, E.E. (1997) The role of diffusion-controlled oscillatory nucleation in the formation of line rock in pegmatite-aplite dikes. Journal of Petrology, 38, 1777–1791.